

International Journal of Multidisciplinary Research and Growth Evaluation.



Antibacterial activity against *Staphylococcus aureus and Salmonella enterica* and Density functional studies on Silver doped Bismuth Selenide nanostructures

M Sarguru ¹, K Sathiyamoorthy ², M Sivasubramanian ³, T Ganesh ⁴, R Thilak Kumar ^{5*}

- ^{1,5} Department of Physics, Periyar Arts College, Thiruvalluvar University, Vellore, Tami Nadu, India
- ² Functional materials and Energy Device Laboratory, Department of Physics and Nanotechnology, SRM IST, Kattankulathur, Chengalpattu, Tamil Nadu, India
- ^{3, 4} Department of Physics, Raja Sarafoji Government College (Autonomous), Thanjavur, Tamil Nadu, India
- * Corresponding Author: R Thilak Kumar

Article Info

ISSN (online): 2582-7138

Volume: 05 Issue: 02

March-April 2024 Received: 08-02-2024 Accepted: 10-03-2024 Page No: 380-386

Abstract

The current study uses a hydrothermal technique to demonstrate the antibacterial activity of silver- doped bismuth selenium nanoparticles. Because they are more biocompatible, nanoparticles made of metals, polymers, or lipids are better suited as antibiotics. They behave like molecules, breaking through bacterial cell membranes to obstruct the molecular process. According to the studies, the activity against bacteria is caused by the host immune system being triggered, RNA and protein synthesis being inhibited, biofilm development being inhibited, cell membrane disruption occurring, or reactive oxygen species (ROS) being produced. Low toxicity and a well-established medicinal agent characterize bismuth. It had the property of good X-ray contrast agent due it is huge atomic mass (Z=83). The human body need selenium as a necessary component. In the present work, the prepared Ag doped bismuth selenide nanostructures are characterized using XRD, HRSEM with EDAX. The antibacterial property of Ag doped bismuth selenide nanostructures against gram-positive bacteria S. aureus and gram negative Salmonella enterica analysed by disk diffusion method. The optimized structure, structural parameters, Homo-Lomo, molecular electrostatic potential, dipole moments, polarizability and hyperpolarazibilary are analyzed using DFT method.

DOI: https://doi.org/10.54660/.IJMRGE.2024.5.2.380-386

Keywords: XRD, HRSEM, EDAX, Antibacterial Activity, DFT

Introduction

One of the most common topological insulators is bismuth selenide (Bi2Se3), which had a energy gap of 0.3 eV. It shows vast applications as the next generation of quantum computing, spintronics and optoelectronics appliances [1]. Moreover, much importance given in the field of physical, chemical and materials science but less use of bismuth selenide nanoparticles in the field of biomedicine. It is interesting to note that selenium (Se) is an important element that it reduces the mortality of prostate, hepatic and pulmonary malignant tumour. Also, bismuth (Bi) is used as a healing agent and has a high coefficient of X-ray attenuation property supporting the potential of Bi2Se3 in biological applications [2]. Silver (Ag) has many uses in the health sector, including as antimicrobial agents, food preservation, textile industries and ecological uses. They require additional uses as antibacterial agents, such as water treatment and the disinfection of household appliances and medical equipment. Furthermore, textile companies have demonstrated the excellent antibacterial activity of silver nanocomposite fabrics, such as cotton fibers infused with silver nano compounds, against germs. The textiles containing silver are advertised, as having the antibacterial properties as well and also the reducing post sweat odour [3]. Chitosan bead hydrogel was observed and encourage a high level of antibacterial activity against *Staphylococcus aureus* and *Salmonella enterica* as well as controlled and extended

drug delivery of silver nano particles. In addition, medical equipment and supplies such scalpels, needles, drainage catheters, venal catheters, and urine catheters are coated with nano silver.

Because of these nanostructures' inherent anti-pathogenic qualities, which have been demonstrated against both planktonic and biofilm-organized microbes, they were created for unusual antibacterial uses. The antibacterial performance of Ag doped Bismuth selenide nanoparticles are improved by the antimicrobial peptide like polymyxin B are used. The production of effective biocompatible Ag nanomaterials with high penetrating power due to the functionalizing molecules like sodium borohydride [4]. Silver nanoparticle functionalization has also been achieved using BSA and PEG. Silver nanoparticles can work better thanks to biofunctionalization, which also increases bioactivity and shields the surface against bacterial invasion from compounds which are derived from plants. The extract of plants such as amides, aldehyde, flavonoids, alkaloids, terpenoids, epicatechins, and catechins and colorants produced the chemicals which are bioactive by specific marine bioresources, such as marine algae [5]. Silver cations are accountable for the bactericidal action of Ag-doped Bismuth selenide nanoparticles. These cations have the ability to attach to the thiol groups of bacterial amino acids in a specific way, interrupting their physiological activity and inducing necrobiosis. By first adhering to the cell surface and altering permeability and respiration, then penetrating the cell barrier and delivering metallic silver ions intracellularly, silver nanoparticles use a Trojan-horse method to carry out their bactericidal action. [6]. So far bismuth selenide nanostructures are synthesized by several methods and for several applications [7-9]. But still some of the investigations are not yet reported. Hence, in the present investigation our aim is to prepare silver doped bismuth selenide nanoparticles for antibacterial activity which helps in the creation of nanostructures with greater potency and a wider range of biological uses in future.

Experimental

To prepare the Ag doped bismuth selenide nanostructures by hydro thermal method, 1mmol of Bi (NO3)35H2O and 1.5mmol Sodium were measured and added into a the beaker and stirred for 1 hour. AgNO3 with several concentrations (5%, 10% and 15%) and labelled as ABS-5%, ABS-10% and ABS-15% solutions were added, after adding pH reducing agents, then it is stirred for several hours The stirred solution kept in the autoclave and tightly closed. It was placed in muffle furnace at 180°C for 24 hours after that it was allowed to cool naturally to reach the RT (room temperature). The synthesized black precipitate was rinsed several times with ethanol and washed many times with deionized water. The sample is collected and dried at 100°C for five hours, then obtained sample is cooled and grinded.

Results and Discussions

XRD Analysis

The crystallinity properties of the synthesized pure and Ag doped bismuth selenide nanostructures are analysed using XRD. The overlayed XRD pattern of the synthesized pure and Ag doped bismuth selenide nanostructures are presented in Fig.1. The peaks are observed in the red shift region for increased concentrations [10]. The nanostructures are in rhombohedral phase with lattice parameters a = 0.4139 and c = 0.4139

= 2.8636 nm and matched very well the JCPDS No. 33-0214 [11]

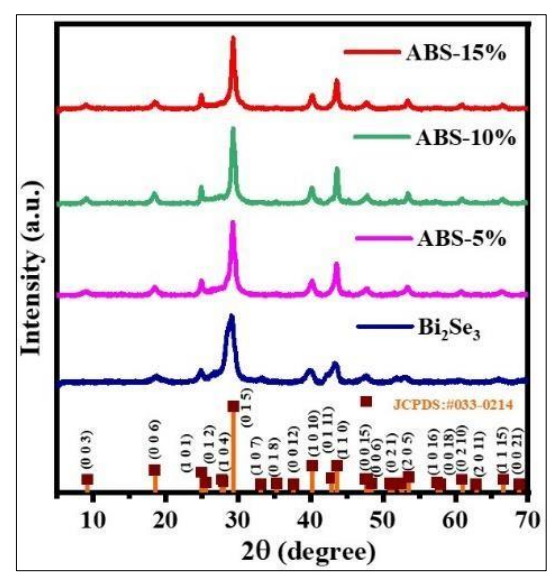


Fig 1: XRD of Ag doped bismuth selenide

HRSEM and EAS Analysis

The morphology of the synthesized silver doped bismuth selenide nanostructures are characterized by HRSEM and is presented in Fig.2. The elemental composition of the synthesized silver doped bismuth selenide nanostructures are analysed using EDAS analysis. The atom % of Se, Ag and Bi are 33.85, 16.33 and 49.82 respectively.

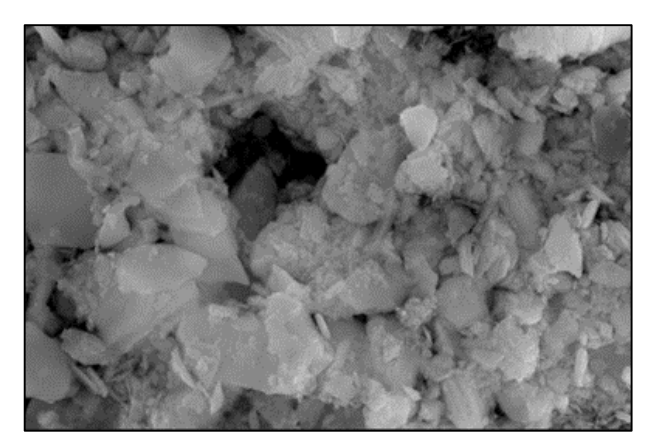


Fig 2: HRSEM of Ag doped Bi₂Se₃

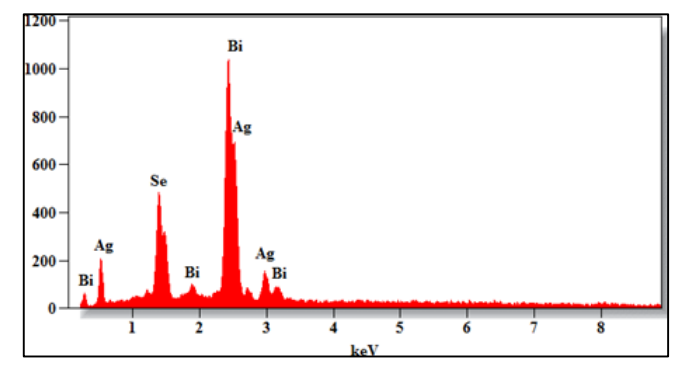


Fig 3: EDAX of Ag doped Bi2Se3

Antibacterial activity and evaluation

Pour, Muller Hinton Agar (MHA) media into the petri dish for bacteria using a sterile swab dampened with the bacterial suspension. If the medium was set then the inoculums were applied to the MHA plates. MHA plates were filled with 20µl of standard antibiotic (ampicillin) disc and sterile samples (disc form). The plates were incubated for twenty-four hours at 37°C. The antibacterial activity was determined by the diameter of zone of inhibition. The average zone of inhibition exhibited by pure bismuth selenide and Ag doped bismuth selenide against Staphylococcus aureus and Salmonella enter ica are presented in Table 1 and 2 respectively and the corresponding pictures are presented in Fig.4 and Fig.5. The pure Bi2Se3 shows the poor antibacterial activity whereas, the silver doped Bi2Se3 NPs shows the good antibacterial activity. The obtained results of the antibacterial study shows the killing efficiency of Ag-doped bismuth selenide nanoparticles increased with increasing concentration of Ag. Antibacterial activity against two bacteria, Salmonella enterica and Staphylococcus aureus which are gram negative and gram positive. When the bacterial cell wall charges get neutralized and permeability of the cytoplasm is changed; subsequently it causes the cell death. The adhesion of Ag doped Bi2Se3 nanoparticles increases the membrane stiffness; changes the cell membrane from order to disorder state and degradable biocomposites like carbohydrates, lipids and amino acids during the killing process [12]. Ag doped bismuth selenide NPs has the ability to attach to the proteins in the plasma membrane. Due to the electrostatic attraction between the negatively charged plasma membrane of the microorganisms and the Ag NPs with positive surface charge; positively charged Ag doped bismuth selenide NPs have stronger antibacterial effects than negatively charged, which can greatly promote the adhesion of Ag-doped Bi2Se3 nanoparticles. Moreover, suppression of sugar metabolism and DNA cleavage or denaturation have been linked to antibacterial action ^[13]. The three-dimensional structure of amnio acids can be altered and active binding sites blocked by these Ag doped nanostructures attaching to the protein's thiol groups (ASH) and creating stable AS-Ag interactions. Consequently, silver ions have the ability to hinder the microbial cells' ability to transport and gives potassium (K+) ions and to prevent the creation of adenosine triphosphate (ATP) ^[14].

The elevated oxidative stress which is linked to the generation of ROS (reactive oxygen species) and ions like H2O2, OH+, O2- and hypochlorous acid are the another harmful impact of the Ag doped bismuth selenide NPs [15]. The organic byproducts of oxygenic metabolism and their intercellular concentrations are low by scrapers such as reduced glutathione (GSH). During oxygenic catabolism, the oxygen gets dissolved, NPs are acts like a catalyst for the production of free radicals. These NPs are interacting with the thiol groups in associated enzymes and glutathione changes into its oxidized GSSG. They can also interfere with the scavenging mechanisms so the quantities of ROS and free radicals are increased [16]. Overabundance of free radicals can directly harm the mitochondrial membrane and disrupt DNA strands when they interact with DNA constituents. Furthermore, elevated ROS levels in the cell cause the plasma membrane, lipids, proteins, and DNA to hyper oxidize. [17].

Table 1: Antibacterial activity of pure Bi2Se3 against Staphylococcus aureus and Salmonella enterica

Zone of inhibition in mm					
S. No	Organism	250μg/ml	500 μg/ml	1000 μg/ml	Standard
1.	Salmonella enterica.	-	7 mm	9 mm	11 mm
2.	Staphylococcus aureus	7 mm	8 mm	10 mm	11 mm

 Table 2: Antibacterial activity of Ag doped Bi2Se3 against Staphylococcus aureus and Salmonella enterica.

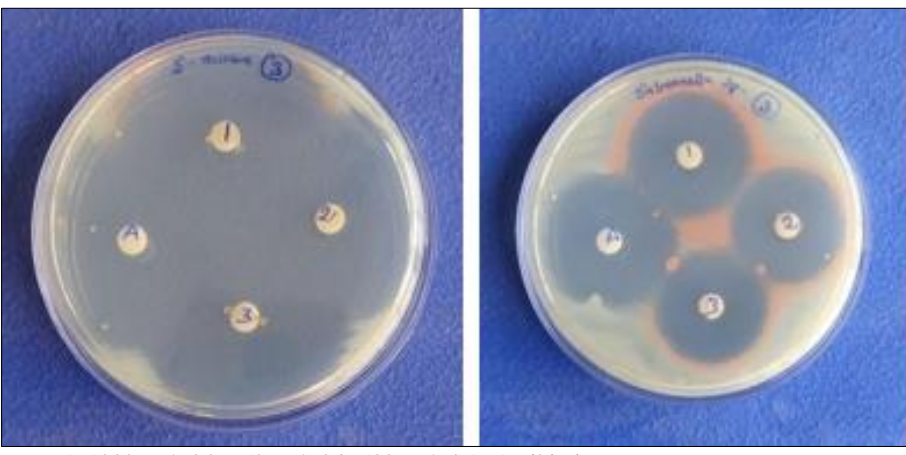
Zone of inhibition in mm					
S. No	Organism	500µg/ml	750 μg/ml	1000 μg/ml	Standard
1	Staphylococcus aureus	17 mm	18 mm	19 mm	18 mm
2	Salmonella enterica.	13 mm	14 mm	15 mm	15 mm



Fig 4a: Staphylococcus aureus



Fig 4b: Salmonella enterica



Note: 1. 1000 μg/ml 2. 750 μg/ml 3. 500 μg/ml A. Antibiotics

Fig 5a: Staphylococcus aureus

Density Functional Studies Molecular geometry

The DFT based vibrational analysis of bismuth selenide and silver doped bismuth selenide were performed using GAUSSIAN program package and the visual inspection was carried out using GAUSSVIEW program [18]. The structures were optimized by assuming C1 point group of symmetry. The molecular structure of bismuth selenide and silver doped bismuth selenide are shown in the Fig.6.The complete molecular geometry of bismuth selenide and silver doped bismuth selenide nano particles were presented in the Table 3. The title compound bismuth selenide consists of 7 atoms with 270 electrons and silver doped bismuth selenide consists of 8 atoms and 314 electrons. Bismuth selenide possesses 15 fundamental modes of vibrations and they are distributed among the symmetry species as: $\square \text{vib} = 11\text{A'}$ (in-plane) + 4A" (out-of-plane) and silver doped bismuth selenide possesses 18 fundamental modes of vibrations and they are distributed among the symmetry species as: $\Box vib = 13A'$ (in-

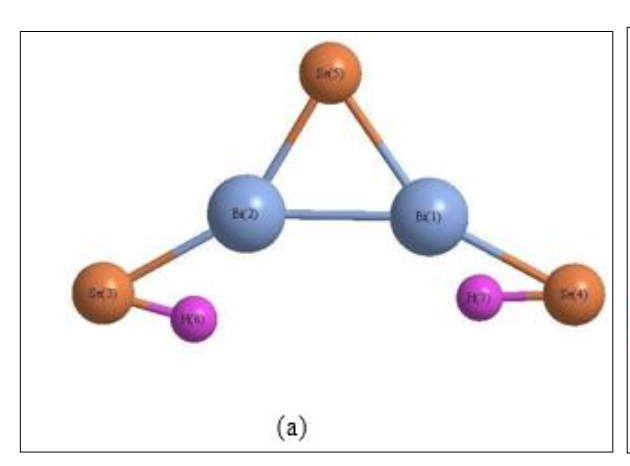
Fig 5b: salmonella enterica

plane)

+ 5A" (out-of-plane). The conformational analysis shows that the global minimum energy of bismuth selenide is 712.78 kJ/mol and silver doped bismuth selenide was 2,355.17 kJ/mol. The conformational analysis revels that doping with silver acquires high energy than the undoped bismuth selenide hence the stability of silver doped bismuth selenide was less than the undoped bismuth selenide.

Homo Lumo Analysis

In the present work HOMO-LUMO analysis were done for bismuth selenide and silver doped bismuth selenide. In the analysis of bismuth selenide, the Highest Occupied Moleuclar Orbit (HOMO) have energy value of -0.16980 eV and Lowest Unoccupied Molecular Orbital have energy value of -0.21291 eV. Energy gap were determined and which was 0.04311 eV. HOMO-LUMO analysis were as shown in the Fig.7.



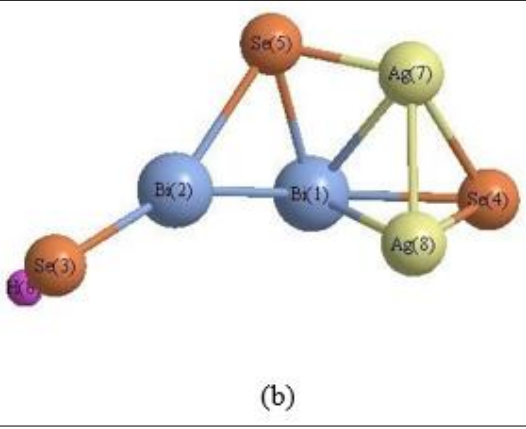


Fig 6: (a) Molecular structure of bismuth selenide (b) Molecular structure of bismuth selenide + Silver

2.5 2.5947

Bismuth selenide Bismuth selenide + Silver Bond length (Å) Bond length (Å) **Parameters Parameters Based on DFT Calculations Based on DFT Calculations** Bi(1)-Se(4) 2.62 Bi(1)-Se(4) 2.6626 Bi(2)-Se(5) 2.62 Bi(2)-Se(5) 2.7821 Bi(2)-Se(3) 2.62 Bi(2)-Se(3) 2.62 Bi(2)-Bi(1) 2.92 Bi(2)-Bi(1) 2.92 2.7822 2.62 Bi(1)-Se(5) Bi(1)-Se(5) Se(3)-H(6) 1.506 1.5059 Se(3)-H(6)2.1574 Se(4)-H(7) 1.506 Se(5)-Ag(7) 2.68 Ag(7)-Ag(8)Ag(7)-Bi(1) 2.742 Bi(1)-Ag(8) 2.8

Table 3: Molecular Geometry of bismuth selenide and silver doped bismuth selenide

Table 4: Bismuth selenide

Se(4)-Ag(8)

Se(4)-Ag(7)

Bismuth selenide		Bismuth selenide+ Silver		
Da	Bond angle (°)	Do	Bond angle (°)	
Parameters	Based on DFT Calculations	Parameters	Based on DFT Calculations	
Se(5)-Bi(2)-Se(3)	150	Se(3)-Bi(2)-Se(5)	152.6791	
Se(5)-Bi(2)-Bi(1)	60	Se(5)-Bi(2)-Bi(1)	54.6419	
Se(3)-Bi(2)-Bi(1)	150	Se(3)-Bi(2)-Bi(1)	152.6789	
Bi(2)-Se(3)-H(6)	44.9903	Bi(2)-Se(3)-H(6)	76.4584	
Bi(2)-Se(5)-Bi(1)	65.3583	Bi(2)-Se(5)-Bi(1)	65.3594	
Se(4)-Bi(1)-Bi(2)	152.6791	Se(4)-Bi(1)-Bi(2)	151.5791	
Se(4)-Bi(1)-Se(5)	152.6791	Se(4)-Bi(1)-Se(5)	152.7791	
Bi(2)-Bi(1)-Se(5)	54.6417	Bi(2)-Bi(1)-Se(5)	53.5417	
H(7)-Se(4)-Bi(1)	30.2079	Ag(7)-Se(4)-Bi(1)	62.8572	
		Ag(7)-Se(4)-Ag(8)	63.4449	
		Bi(1)-Se(4)-Ag(8)	65.602	
		Ag(8)-Bi(1)-Ag(7)	57.8281	
		Ag(8)-Bi(1)-Se(5)	89.9988	
		Ag(8)-Bi(1)-Se(4)	54.4005	
		Ag(8)-Bi(1)-Bi(2)	79.9997	
		Ag(7)-Bi(1)-Se(5)	47.3834	

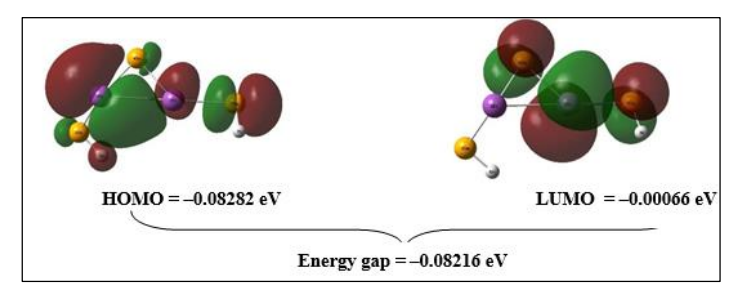


Fig.7: HOMO-LUMO of bismuth selenide

In the analysis of silver doped bismuth selenide, the Highest Occupied Moleuclar Orbit (HOMO) have energy value of – 0.14932 eV and Lowest Unoccupied Molecular Orbital have energy value of –0.20780 eV. Energy gap were determined

and which was -0.05848 eV which was very smaller in value and means that the title compound has better stability. HOMO-LUMO analysis were as shown in the Fig.8.

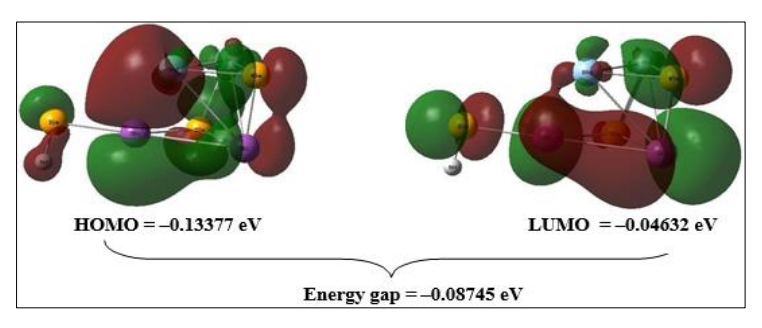


Fig 8: HOMO-LUMO of silver doped bismuth selenide

There was a difference in energy gap due to substitution of silver in bismuth selenide. Before substitution, the energy gap was 0.04311 eV and after substitution, the energy gap was 0.05848 eV. It clearly shows the energy gap increases with the value of 0.01537 eV due to the doping of silver [19].

Molecular electrostatic potential Analysis

The MEP of bismuth selenide and silver doped bismuth selenide were computed at the B3LYP/6-31G** level of optimised geometry to compute reactive sites for nucleophilic and for an electrophilic assault on the molecule. Fig. 9 and Fig.10 shows how the negative (red) areas of MEP are associated to electrophilic reactivity whereas the positive (blue) portions are associated to nucleophilic reactivity in bismuth selenide and silver doped bismuth selenide respectively.

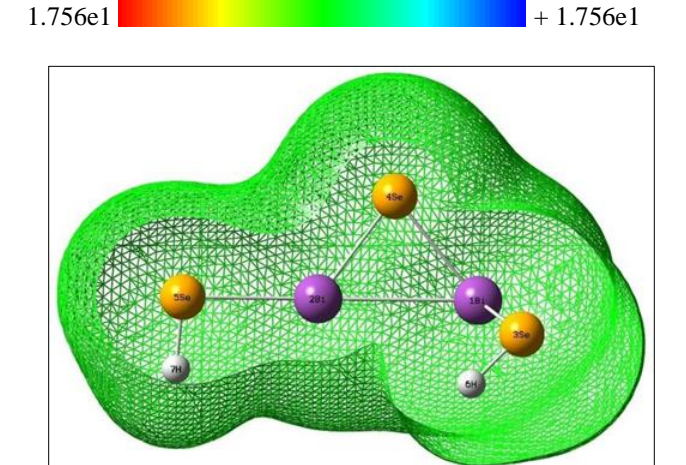


Fig 9: Molecular Electrostatic Potential of bismuth selenide

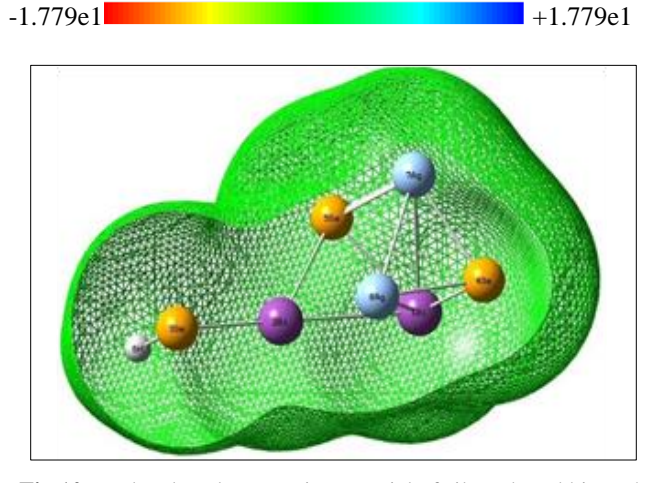


Fig 10: Molecular Electrostatic Potential of silver doped bismuth selenide

The Molecular Electrostatic Potential (MEP) is connected to the electronic density, hence it is a useful descriptor for determining the positions for electrophilic assault, nucleophilic reactions, and hydrogen-bonding interactions. The extreme limits of the electron density observed in silver doped bismuth selenide are $-1.779e1 \, \text{Å}^{-1}$ (red) and $+1.779e1 \, \text{Å}^{-1}$ (blue). (Here $1 \, \text{eÅ}^{-1} = 332.1 \, \text{kcal·mol}^{-1}$). In the MEP analysis, green colour represents the potential halfway between the two extremes (red/dark blue). The green regions shows the location of the mean potential in both silver doped

bismuth selenide and in bismuth selenide [20].

Polarizability and Hyperpolarizability analysis

The Dipole Moment, polarizability and hyperpolarizability analysis [21] has been carried out for bismuth selenide and silver doped bismuth selenide on the basis of density functional theory are presented in the Table 4 and Table 5 respectively.

Table 5: Dipole moments, Polarizability values of bismuth selenide

Components	Parameter	Values Calculated using B3LYP/6-31G** in a.u.
Dinala Mamant	$\Box \mathbf{x}$	0.549
Dipole Moment Components	$\Box \mathbf{y}$	0.975
Components	$\Box z$	-0.015
Total Dipole Moment		1.121
	$\Box xx$	351.836
	□yy	-8.774
Doloniashility sommonants	\Box zz	176.95
Polarizability components	□xy	65.768
	□yz	-12.688
	□xz	41.277
Total Polarizability	□tot	614.368
Static Polarizability		879210.378
	βxxx	91.263
	βхху	-16.943
	βхуу	-22.622
II	βууу	-16.149
Hyper polarizability	βxxz	-93.599
Components	βxyz	-62.443
	βууz	82.321
	βxzz	-11.366
	βyzz	-10.545
	βzzz	335.657
Hyperpolarizability		332.275

Table 6: Dipole moments, Polarizability values of Silver doped bismuth selenide

Components	Parameter	Values Calculated using B3LYP/6-31G** in a.u.
D' 1 M	$\Box \mathbf{x}$	0.834
Dipole Moment	□y	0.293
Components	$\Box z$	-0.195
Total Dipole Moment		0.905
	$\Box xx$	288.958
	□yy	-3.337
Polarizability	\Box zz	158.345
components	$\Box xy$	95.968
	□yz	-10.688
	$\Box xz$	253.231
Total Polarizability	□tot	782.477
Static Polarizability		523324.455
	βxxx	1430.591
	βxxy	-448.003
	βхуу	539.308
	βууу	-576.007
Hyper polarizability	βxxz	-334.959
Components	βxyz	-92.513
	βууz	282.011
	βxzz	1134.938
	βyzz	-299.296
	βzzz	685.934
Hyperpolarizability		3433.02

From the dipole moment analysis, the calculated total dipole moment value for bismuth selenide is 1.121 a.u. and for silver doped bismuth selenide the total dipole moment is 0.905 a.u respectively. That is the total dipole moment decreased by 0.216 a.u due to the silver dopant.

The calculated value of static polarizability for bismuth selenide is 879210.378 a.u. whereas the calculated value of static polarizability for silver doped bismuth selenide is 523324.455 a.u. i.e., having the variation of 355885.923 a.u. The calculated Hyperpolarizability for bismuth selenide is 332.275 a.u. whereas the silver doped bismuth selenide possesses 3433.02 a.u. which is having the difference of 3100.745 a.u.

Conclusion

Both pure and Ag-doped bismuth selenide are synthesised via convenient hydrothermal technique. The crystalline parameters of the undoped and silver doped bismuth selenide are characterized using XRD and with increasing the concentration the peaks are observed in the red shift region. Morphological structures shows that the NPs are nanoflakes exhibited by HRSEM and EDAX pattern confirms the elemental presentation. The antibacterial activity of Ag doped bismuth selenide nanostructures is analysed against gram positive Staphylococcus aureus and gram negative Salmonella enterica by disk diffusion method. Ultimately the results of Ag doped Bi2Se3 nanostructures shows more effective antibacterial for gram positive bacteria than gram negative bacteria. In addition that DFT method is applied for the pure and Ag doped bismuth selenide nanostructures. The energy band gap of pure bismuth selenide and Ag doped bismuth selenide are -0.08216 eV and -0.08745 eV respectively. Also, it is observed that the calculated values of dipole moment, polarizability and hyperpolarizability values are greater than that of pure bismuth selenide.

References

- Batool Z, Bashir S, Ismail M, Kousar R, Manzoor MZ, Khan HM, Kalsoom A. Synthesis, structural, optical, and dielectric properties of novel barium-doped bismuth selenide. Journal of Materials Science: Materials in Electronics. 2022;33(21):17212-17222.
- Fang MC, Go AS, Chang Y, Borowsky LH, Pomernacki NK, Udaltsova N. A new risk scheme to predict warfarin-associated hemorrhage: The ATRIA (Anticoagulation and Risk Factors in Atrial Fibrillation) Study. Journal of the American College of Cardiology. 2011;58(4):395-401.
- 3. Angajala G, Pavan P, Subashini R. Lipases: An overview of its current challenges and prospectives in the revolution of biocatalysis. Biocatalysis and Agricultural Biotechnology. 2016;7:257-570.
- Keshari AK, Kumar R. Nanostructured MoS2-, SnS2-, and WS2-Based Anode Materials for High-Performance Sodium-Ion Batteries via Chemical Methods: A Review Article. Energy Technology. 2021;9(8):2100179.
- Kora AJ, Arunachalam J. Assessment of antibacterial activity of silver nanoparticles on Pseudomonas aeruginosa and its mechanism of action. World Journal of Microbiology and Biotechnology. 2011;27:1209-16.
- 6. Ramalingam B, Parandhaman T, Das SK. Antibacterial effects of biosynthesized silver nanoparticles on surface ultrastructure and nanomechanical properties of gramnegative bacteria viz. Escherichia coli and Pseudomonas

- aeruginosa. ACS applied materials & interfaces. 2016;8(7):4963-76.
- 7. Duering M, Biessels GJ, Brodtmann A, Chen C, Cordonnier C, de Leeuw FE. Neuroimaging standards for research into small vessel disease—advances since 2013. The Lancet Neurology. 2023;22(7):602-618.
- 8. Kim CJ, Romero R, Chaemsaithong P, Chaiyasit N, Yoon BH. Acute chorioamnionitis and funisitis: definition, pathologic features, and clinical significance. American journal of obstetrics and gynecology. 2015;213(4):S29-S52.
- 9. Wang W, Xu Y, Gao R, Lu R, Han K, Wu G. Detection of SARS-CoV-2 in different types of clinical specimens. Journal of the American Medical Association More at Abbreviations.com. 2020;323(18):1843 1844.
- 10. Hegde GS, Prabhu AN, Yang CN, Kuo YK. Materials Chemistry and Physics. 2022;278:125675. Available from:
 - https://doi.org/10.1016/j.matchemphys.2021.125675
- 11. Kulsi C, Ghosh A, Mondal A, Kargupta K, Ganguly S, Banerjee D. Remarkable photo-catalytic degradation of malachite green by nickel doped bismuth selenide under visible light irradiation. Applied Surface Science. 2017;392:540-548.
- 12. Rajesh S, Koshi E, Philip K, Mohan A. Antimicrobial photodynamic therapy: An overview. Journal of Indian Society of Periodontology. 2011;15(4):323-327.
- 13. Ghosh S, May MJ, Kopp EB. NF-κB and Rel proteins: evolutionarily conserved mediators of immune responses. Annual review of immunology. 1998;16(1):225-260.
- 14. Schreurs WJ, Rosenberg H. Effect of silver ions on transport and retention of phosphate by Escherichia coli. Journal of Bacteriology. 1982;152(1):7-13.
- 15. Rinna A, Magdolenova Z, Hudecova A, Kruszewski M, Refsnes M, Dusinska M. Effect of silver nanoparticles on mitogen-activated protein kinases activation: role of reactive oxygen species and implication in DNA damage. Mutagenesis. 2015;30(1):59-66.
- Ahearn DG, May LL, Gabriel MM. Adherence of organisms to silver-coated surfaces. Journal of Industrial Microbiology and Biotechnology. 1995;15(4):372-376.
- 17. Lok CN, Ho CM, Chen R, He QY, Yu WY, Sun H. Proteomic analysis of the mode of antibacterial action of silver nanoparticles. Journal of proteome research. 2006;5(4):916-924.
- 18. Curtiss LA, Redfern PC, Raghavachari K. Gaussian-4 theory. The Journal of chemical physics. 2007, 126(8).
- 19. Miyazaki S, Shirakawa H, Nakada K, Honda Y. Essential role of the inositol 1, 4, 5-trisphosphate receptor/Ca2+ release channel in Ca2+ waves and Ca2+ oscillations at fertilization of mammalian eggs. Developmental biology. 1993;158(1):62-78.
- 20. Champagne BJ, O'Connor LM, Ferguson M, Orangio GR, Schertzer ME, Armstrong DN. Efficacy of anal fistula plug in closure of cryptoglandular fistulas: long-term follow-up. Diseases of the colon & rectum. 2006;49:1817-1821.
- Raghavachari K, Saha A. Accurate composite and fragment-based quantum chemical models for large molecules. Chemical Reviews. 2015;115(12):5643-5677.